ELSEVIER

Contents lists available at ScienceDirect

International Journal of Pharmaceutics

journal homepage: www.elsevier.com/locate/ijpharm





Enhancing physical and chemical stability of hygroscopic hydroxytyrosol by cocrystal formation

Bingqing Zhu^{a,1}, Mengyuan Xia^{a,b,1}, Zhenfeng Ding^{a,b}, Xiaoyi Rong^a, Xuefeng Mei^{a,b,*}

- ^a Pharmaceutical Analytical & Solid-State Chemistry Research Center, Shanghai Institute of Materia Medica, Chinese Academy of Sciences, 555 Zuchongzhi Road, Shanghai 201203, China
- b University of Chinese Academy of Sciences, No. 19A Yuquan Road, Beijing 100049, China

ARTICLE INFO

Keywords: Hydroxytyrosol Cocrystal Solidification Hygroscopicity Stability

ABSTRACT

Hydroxytyrosol (HT) is a natural phenolic compound with potent antioxidant activity extracted from olive trees. It is generally a slightly hydrated viscous liquid at ambient conditions, and it is highly susceptible to oxygen due to the presence of catechol moiety. Although encapsulation technique provides HT in powder form, it does not improve its chemical stability. Herein, we propose an efficient solution to the high hygroscopicity and poor stability of HT. Four cocrystals were first reported, and their intermolecular interactions were analyzed in detail. After cocrystallization, the melting point is increased and the hygroscopicity is significantly decreased. HT cocrystals are thus solid at room temperature. Moreover, hydroxytyrosol cocrystals with betaine (HT-BET) and nicotinamide (HT-NIC) demonstrate superior chemical stability than pure HT, olive extract, and HT encapsulation material. Therefore, cocrystallization can be considered as a promising approach to overcome the application obstacles of HT.

1. Introduction

The Mediterranean diet (MD) is associated with a lower incidence of cardiovascular diseases ((Rosato et al., 2019)), neurological diseases, and certain types of cancer ((Mentella et al., 2019)). The potential health benefits are reported to be related to the dietary consumption of olive oil and its phenolic compounds, in particular of oleuropein (OLE), secoiridoid (SEC), and hydroxytyrosol (HT) ((Loizzo et al., 2011; Lopez de las Hazas et al., 2018)). Both OLE and SEC are hydrolyzed to HT after absorption ((Gonzalez et al., 2019; Lopez de las Hazas et al., 2016)). In recent years, HT has received increasing attention due to its potent antioxidant activity and multiple pharmacological activities. Moreover, HT is the only polyphenol recognized by the European Food Safety Authority (EFSA) that can protect low-density lipoprotein (LDL) from oxidative damage ((Galmes et al., 2021)). Although HT shows broad application prospects in functional foods, cosmetics, and even medicine ((Gullon et al., 2020)), it cannot be used directly in many cases in that pure HT is easy to absorb water and generally appears as a sticky liquid at room temperature. Moreover, the presence of catechol moiety results in the extremely instability of HT to oxygen ((Monteiro et al., 2021)).

For now, there are two commercial powdered HT ingredients, one is encapsulated HT with about 20–30 % loading, and the other is olive leaf extract which contains about 20 % HT. However, their stability is still unsatisfactory. To answer the current nutraceutical industrial demand, there is an urgent need for developing an adequate formulation to overcome these issues related to poor physical and chemical stability.

Cocrystallization has great potential to improve the physicochemical properties of active ingredients without altering their molecule structure and bioactivity (Guo et al., 2021; Bolla et al., 2022; (Bofill et al., 2021; Dias et al., 2021; Wang et al., 2018)). In this work, we expect to address the physical and chemical stability issues of HT through cocrystallization. The phenolic hydroxyl group of HT was selected for supramolecular synthon design and coformers containing carboxylic anion, carboxylic acid, amide and pyridine groups were screened for HT cocrystals (Fig. S1). Three novel cocrystals of HT with betaine (BET), nicotinamide (NIC), and isonicotinamide (INA) were obtained, wherein HT-INA has two polymorphs, namely HT-INA Form I and HT-INA Form II. The solubility of this cocrystals is above 10 mg/mL. When administered, these cocrystals will dissolve and substantial dissociation of HT from its cocrystals occurs before absorption. Therefore, the

^{*} Corresponding author at: Pharmaceutical Analytical & Solid-State Chemistry Research Center, Shanghai Institute of Materia Medica, Chinese Academy of Sciences, 555 Zuchongzhi Road, Shanghai 201203, China (X. Mei).

E-mail address: xuefengmei@simm.ac.cn (X. Mei).

¹ These authors contributed equally to this work and should be considered co-first authors.

pharmacological activity of these cocrystals remains unchanged. Properties including melting point, hygroscopicity and chemical stability were evaluated for these cocrystals.

2. Materials and methods

2.1. Materials

Hydroxytyrosol with a purity greater than 98 % was purchased from Hangzhou Viablife Biotech Co., Ltd. (Zhejiang, China). The melting point of HT is about 54 °C and it is fluffy solid in a dry environment. However, it becomes sticky liquid after slightly water absorption under ambient condition. Encapsulated HT powder with about 29 % HT loading and olive leaf extract which contains about 26 % HT were purchased from Shanxi Fuheng Biotechnology Co., Ltd. (Shanxi, China). Nicotinamide with a purity greater than 98 % was purchased from J&K Scientific Ltd. (Beijing, China). Isonicotinamide with a purity greater than 99 % was purchased from Shanghai Aladdin Bio-Chem Technology Co., Ltd. (Shanghai, China). Betaine (purity > 98 %) and all solvents used in this work were purchased from Sinopharm Chemical Reagent Co., Ltd. (Shanghai, China).

2.2. Synthesis of cocrystal HT-BET

617 mg HT (4 mmol) and 469 mg betaine (4 mmol) were added to 20 mL of mixed solvents of methanol and isoamylol (1: 1, v/v) and stirred at 40 °C until clear. The solution was then transferred to -20 °C to allow recrystallization. After 24 h, block-shaped single crystals were obtained.

2.3. Synthesis of cocrystal HT-NIC

617 mg HT (4 mmol) and 488 mg nicotinamide (4 mmol) were added to 20 mL ethanol and stirred at 40 °C until clear. The solution was then transferred to -20 °C to allow recrystallization. After 24 h, block-shaped single crystals were obtained.

2.4. Synthesis of HT-INA Form I

617 mg HT (4 mmol) and 488 mg isonicotinamide (4 mmol) were added to 20 mL of ethyl acetate and stirred at 40 °C until clear. The solution was then transferred to -20 °C to allow recrystallization. After 24 h, block-shaped single crystals were obtained.

2.5. Synthesis of HT-INA Form II

Bulk powders of HT-INA Form II were prepared by liquid-assisted grinding using XM-2017S oscillatory ball mill (Shanghai Jingxin Industrial Development Co., Ltd., Shanghai, China) with teflon grinding jars (50 mL). 200 μ L of ethyl acetate was added to a mixture of HT (4 mmol) and INA with a molar ratio of 1:1, and the materials were ground at a frequency of 40 Hz for 1 h. Powder of HT-INA Form II was added as seed to the saturated solution of ethyl acetate containing equal molar ratios of HT (4 mmol, 617 mg) and INA (4 mmol, 488 mg). After cooling at $-20~{}^{\circ}\text{C}$ for 24 h, block-shaped crystals were obtained.

2.6. Powder X-ray diffraction (PXRD)

PXRD patterns were collected using a Bruker D8 Advance X-ray diffractometer (Cu K α radiation). The tube voltage and current of the generator were set to 40 kV and 40 mA, respectively. The samples were measured with a continuous scan at 0.1 s step $^{-1}$ in the 3-40 $^{\circ}$ 20 range with a step size of 0.02 $^{\circ}$. Data were imaged and integrated with RINT Rapid, and peaks were analyzed with Jade 6.0 from Ragaku.

Table 1Crystallographic data of HT and HT cocrystals.

	HT-BET	HT-NIC	HT-INA Form I	HT-INA Form II
Formula	C ₁₃ H ₂₁ NO ₅	C ₁₄ H ₁₆ N ₂ O ₄	C ₁₄ H ₁₆ N ₂ O ₄	C ₁₄ H ₁₆ N ₂ O ₄
Crystal system	Monoclinic	Monoclinic	Monoclinic	Monoclinic
Space group	Cc	$P2_{1/n}$	C2/c	$P2_{1/n}$
Temperature (K)	170	170	170	170
a (Å)	13.549 (6)	9.4999 (17)	19.896 (6)	7.1956 (2)
b (Å)	13.467 (6)	11.8285 (17)	5.4771 (19)	18.9983 (6)
c (Å)	9.326 (4)	11.4439 (17)	26.557 (10)	9.6869 (3)
α (deg)	90	90	90	90
β (deg)	124.166	96.628 (6)	107.894	95.9670
	(12)		(10)	(10)
γ (deg)	90	90	90	90
$V(\mathring{A}^3)$	1407.9 (11)	1277.4 (3)	2753.9 (17)	1317.06 (7)
$D_{\rm Cal}~({\rm g/cm}^3)$	1.280	1.422	1.333	1.393
Z	4	4	8	4
λ (Mo-Kα)	0.71073	0.71073	0.71073	0.71073
Independent reflns	2069	2612	2796	2689
GooF	0.945	1.015	1.012	1.004
Rint	0.0816	0.0770	0.0738	0.0646
R_1	0.0617	0.0520	0.0622	0.0444
wR_2	0.1792	0.1443	0.1497	0.1103
CCDC number	2,269,517	2,269,518	2,269,519	2,269,520

2.7. Single Crystal X-ray diffraction (SCXRD)

SCXRD data were collected using a Bruker Apex II CCD diffractometer using Mo-K α radiation ($\lambda=0.71073$ Å) at 170 K. Integration and scaling of intensity data was performed using the SAINT program (Sheldrick, 1995). All data were corrected for absorption effects using SADABS. The structures were solved by direct method and refined with the full-matrix least-squares technique through SHELX-2014 software. Non-hydrogen atoms were refined with anisotropic displacement parameters, and hydrogen atoms were placed in the calculated positions and refined with a riding model. Crystallographic data and refinement details are listed in Table 1.

2.8. Thermogravimetric analysis (TGA)

TGA experiments were conducted on a TGA-55 equipment (TA Instruments). Each sample (5–10 mg) was placed in an open aluminum oxide pan and heated from 25 °C to 410 °C at 10 °C $\rm min^{-1}$. Nitrogen was used as the purge gas at a flow rate of 40 mL $\rm min^{-1}$.

2.9. Differential scanning calorimetry (DSC)

DSC experiments were performed on a PerkinElmer DSC 8500 instrument. Accurately weighed samples (3–5 mg) were heated in sealed non-hermetic aluminum pans at a heating rate of $10\ ^{\circ}\text{C}\ \text{min}^{-1}$ under nitrogen gas flow of 50 mL min $^{-1}$ purge. Two-point calibration using indium and tin was carried out to check the temperature axis and heat flow of the equipment.

2.10. Dynamic vapor sorption (DVS)

The hygroscopicity behaviors of the materials were studied on an Intrinsic DVS instrument from Surface Measurement Systems, Ltd. The samples were mounted on a balance and studied over a humidity range from 0 to 95 % RH at 25 $^{\circ}\text{C}$. Each humidity step was made if less than a 0.02 % weight change occurred within 10 min.

2.11. Stability study

The chemical stability of HT, HT-BET, HT-NIC, encapsulated HT and

Fig. 1. (a) Supramolecular synthons for cocrystal design, (b) Chemical structures of HT and coformers.



Fig. 2. Physical appearances of HT and HT cocrystals at room temperature: (a) solid HT, (b) liquid HT, (c) HT-BET, (d) HT-NIC, (e) HT-INA Form I, and (f) HT-INA Form II.

olive leaf extract under high temperature (60 °C), high humidity (75 % RH, saturated sodium chloride solution) and accelerated conditions (40 °C/75 % RH) were investigated. Samples were taken out at regular exposure intervals to determine HT assay (0, 2, 4, 7, 10 and 14 days under thermal and high humidity conditions, and 0, 0.5, 1, 2, 3 and 6 months under accelerated condition). Samples for high humidity study were laid out in open bottles, and for thermal and accelerated studies were sealed in double layer polyethylene bags.

2.12. Water content determination

The water content during high humidity stability tests were determined using a Mettler Toledo C20 Coulometric KF Titrator.

2.13. High-Performance liquid chromatography (HPLC)

HT was quantified using an Agilent 1260 series HPLC from Agilent Technologies Co., Ltd., equipped with a quaternary pump (G1311C), a diode-array detector (G1315D) set to 280 nm, and a 4.6×150 mm, $5~\mu m$ Agilent Eslipse Plus C18 column. A gradient method using water with 0.1 % (v/v) trifluoroacetic acid (eluent A) and acetonitrile (eluent B) was run under a flow rate of $1.0~mL~min^{-1}$. The column temperature was set to 35 °C, and the injection volume was 20 μL . The gradient elution procedure started with 95 % A and was kept for 10 min. Then it decreased to 50 % within 1 min and held for another 3 min, and then rapidly returned to 95 % A in 0.1 min and held for 2.9 min for reequilibrium. All samples were dissolved in water containing 0.1 % (v/v) trifluoroacetic acid to avoid HT degradation in solution before HPLC analysis.

3. Results and discussion

3.1. Cocrystal preparation and PXRD analysis

In this work, four novel multi-component crystals of HT, including HT-betaine (HT-BET), HT-nicotinamide (HT-NIC), HT-isonicotinamide

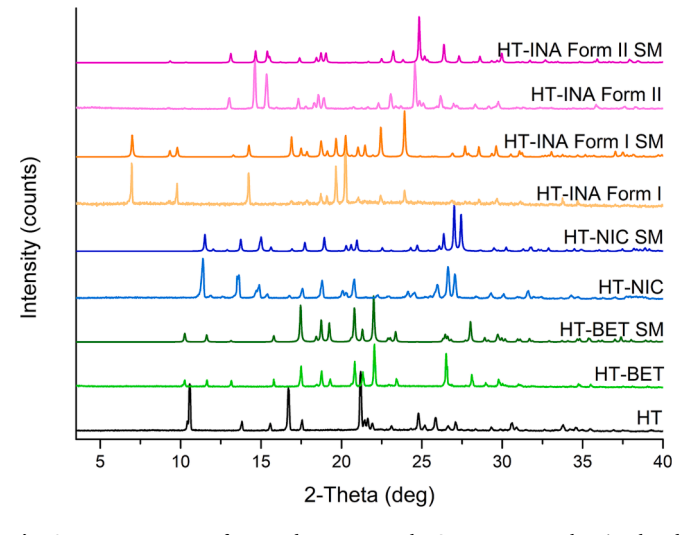


Fig. 3. PXRD patterns of HT and HT cocrystals. SM represents the simulated PXRD patterns.

Form I (HT-INA Form I), and HT-isonicotinamide Form II (HT-INA Form II), were obtained (Fig. 1). Bulk HT-BET, HT-NIC and HT-INA Form I were obtained by cooling from solution and HT-INA Form II was prepared by liquid-assisted grinding. Although pure HT is a yellow fluffy solid in a dry environment (Fig. 2a), a deliquescence behavior can be observed and it converts to oily liquid at ambient condition (Fig. 2b). This unsatisfactory property greatly limits its application in dietary supplement. After cocrystallization, HT is converted to white to offwhite powder (Fig. 2c-2f) with good flowability at room temperature.

PXRD analysis was used to identify cocrystal formation by comparing the diffraction patterns of cocrystals and the respective starting materials. The PXRD patterns of HT, HT-BET, HT-NIC, HT-INA Form I and HT-INA Form II are shown in Fig. 3. All synthesized cocrystals display distinct PXRD patterns to HT and the coformers (Fig. S2), confirming the

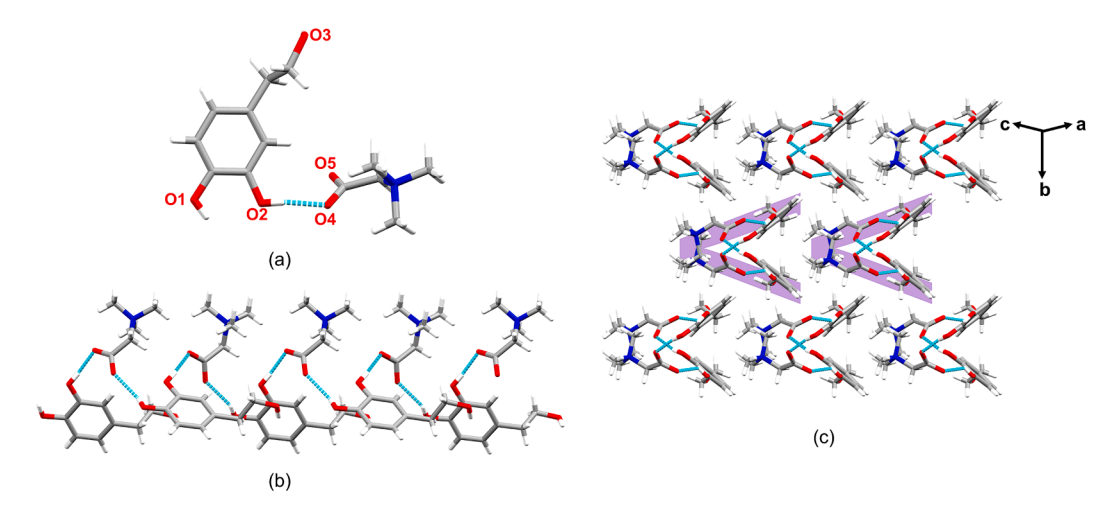


Fig. 4. Crystal structure of HT-BET cocrystal: (a) asymmetric unit, (b) BET molecules behavior as bridge to link HT molecules, and (c) 3D structure. The V-shaped unit is highlighted in purple. (For interpretation of the references to colour in this figure legend, the reader is referred to the web version of this article.)

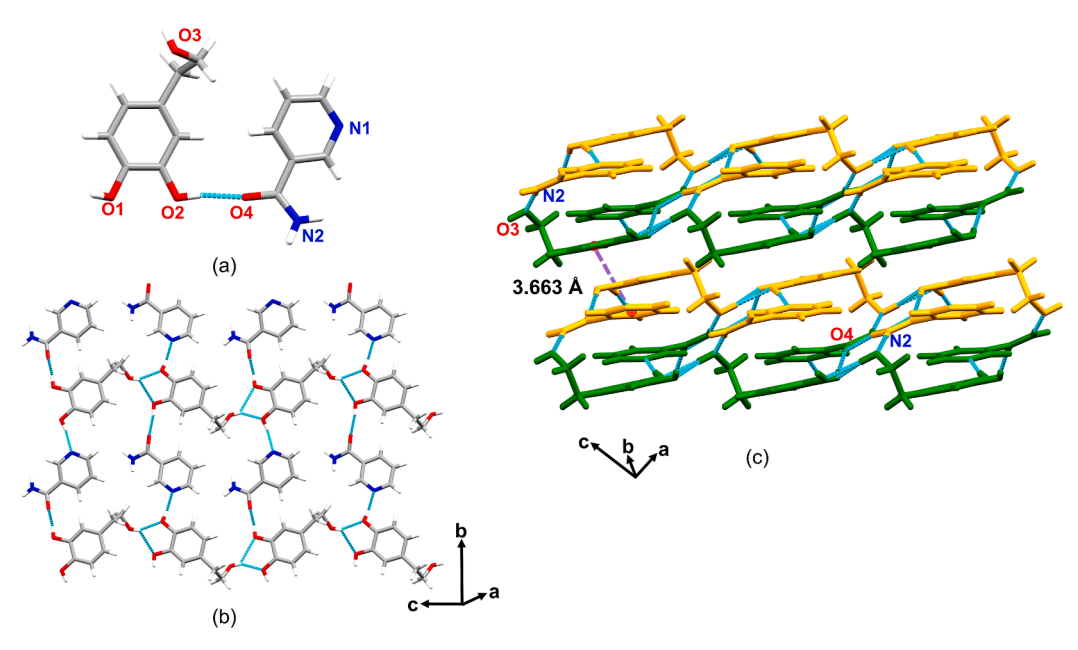


Fig. 5. Crystal structure of HT-NIC cocrystal: (a) asymmetric unit, (b) HT and NIC are connected to give a 2D layer, and (c) 2D layers packed through $\pi...\pi$ interactions and van der Waals forces to give a 3D architecture. Different 2D layers are highlighted in yellow and green. (For interpretation of the references to colour in this figure legend, the reader is referred to the web version of this article.)

formation of new phases. In addition, phase purity of the cocrystals were confirmed by comparing the experimental PXRD patterns with the simulated PXRD patterns calculated from SCXRD analysis. It is noted that peak shifts occur between calculated and experimental pattern of HT-NIC, especially in the range of 25-30°. This can be attributed to the thermal lattice expansion between 170 K (test temperature of SCXRD) and 298 K (test temperature of PXRD).

3.2. Single Crystal structures

3.2.1. HT-BET cocrystal

Block-shaped single crystals of HT-BET were obtained by cooling from mixed solvents of methanol and isoamylol at -20 °C. The crystal structure of HT-BET is solved in a monoclinic Cc space group, containing one HT molecule and one BET molecule in the asymmetric unit, and they interact with each other through O_2 -H····O₄ (d=2.645 Å) hydrogen bond (Fig. 4a). Each BET molecule functions as a bridge to link two HT molecules through O_2 -H····O₄ (d=2.645 Å) and O_1 -H····O₅ (d=2.732 Å)

hydrogen bonds to form a "V" type chain, as shown in Fig. 4b. The "V"-shaped chains are further stacked via van der Waals forces to form the three-dimensional (3D) structure of HT-BET, as shown in Fig. 4c.

3.2.2. HT-NIC cocrystal

Block-shaped single crystals of HT-NIC were obtained by cooling from ethanol at -20 °C. The crystal structure of HT-NIC is solved in a monoclinic $P2_1/n$ space group, containing one HT molecule and one NIC molecule in the asymmetric unit (Fig. 5a). HT molecules and NIC molecules are connected with each other through $O_2\text{-H}\cdots O_4$ (d = 2.742 Å) and $O_3\text{-H}\cdots N_1$ (d = 2.770 Å) to form 1D chains. These neighbored chains are linked in anti-parallel fashion by $O_1\text{-H}\ldots O_3$ (d = 2.837 Å) hydrogen bond between two HT molecules, forming 2D layers (Fig. 5b). The 2D layers are further connected by $N_2\text{-H}\cdots O3$ (d = 2.861 Å) and $N_2\text{-H}\cdots O4$ (d = 2.963 Å) hydrogen bonds, and then packed through $\pi\ldots\pi$ interactions (dcentroid...centroid = 3.663 Å) and van der Waals forces to the 3D structure (Fig. 5c).

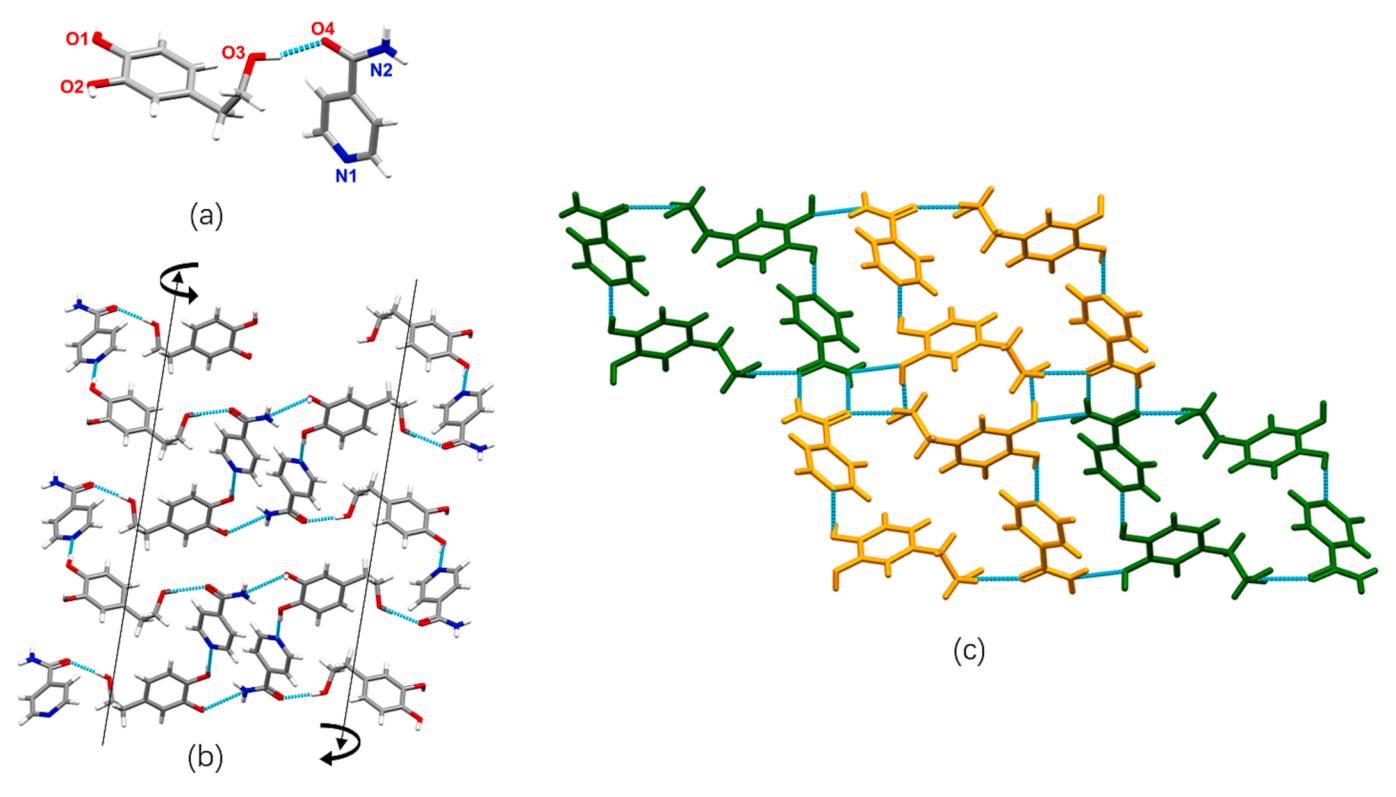


Fig. 6. Crystal structure of HT-INA Form I: (a) asymmetric unit, (b) two left/right-handed helical chains, (c) adjacent chains (highlighted in green and yellow) are inversion-connected to give 3D architecture. (For interpretation of the references to colour in this figure legend, the reader is referred to the web version of this article.)

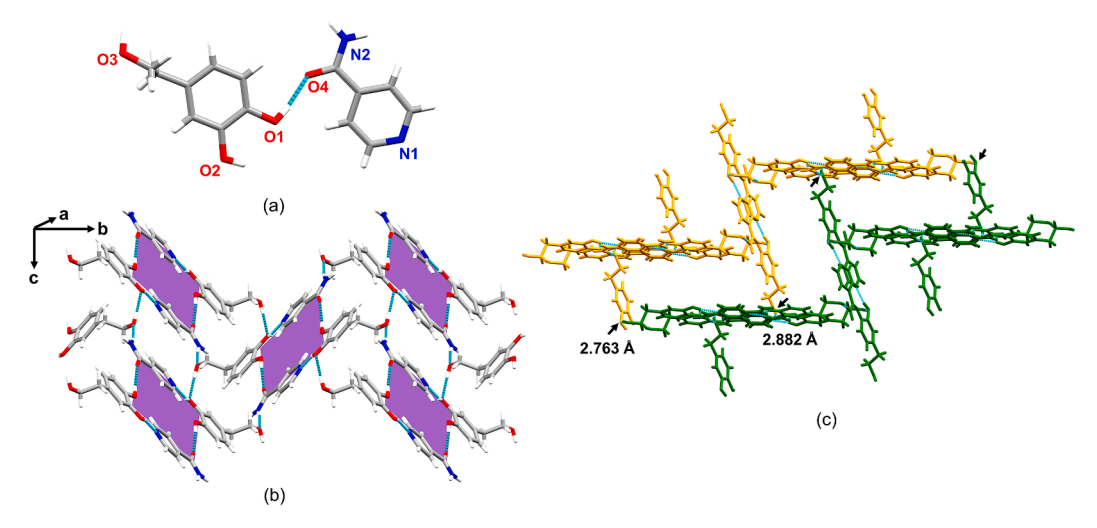


Fig. 7. Crystal structure of HT-INA Form II: (a) asymmetric unit, (b) a serrated 2D layer parallel to the bOc plane, and (c) 2D layers stack through O_3 -H··· O_2 and N_2 -H··· O_3 hydrogen bonds to give a 3D architecture (yellow and green represent different 2D layers). (For interpretation of the references to colour in this figure legend, the reader is referred to the web version of this article.)

3.2.3. HT-INA Form I cocrystal

Block-shaped single crystals of HT-INA Form I were obtained by cooling from ethyl acetate at -20 °C. The crystal structure of HT-INA Form I is solved in a monoclinic C2/c space group, and the asymmetric unit contains one HT molecule and one INA molecule (Fig. 6a). HT and INA molecules are arranged in a head-to-tail fashion through O₃-H···O₄ (d = 2.721 Å) and O₁-H···N₁ (d = 2.808 Å) hydrogen bonds, forming left/right-handed helical chain structures along b axis (Fig. 6b). The adjacent opposite helical chains are inversion-related by means of O₂-H···O₃ (d = 2.666 Å) hydrogen bond and amide homosynthon (N₂-H···O₄, d = 3.036 Å), giving a three-dimensional architecture (Fig. 6c).

3.2.4. HT-INA Form II cocrystal

Block-shaped single crystals of HT-INA Form II were obtained by cooling from ethyl acetate at -20 °C with the aid of seed. The crystal structure of HT-INA Form II was solved in a monoclinic $P2_{1/n}$ space group, and the asymmetric unit contains one HT molecule and one INA molecule, which are connected via $O_1\text{-H}\cdots O_4$ (d = 2.686 Å) hydrogen bond (Fig. 7a). The two asymmetric units are interacted through $O_2\text{-H}\cdots N_1$ (d = 2.722 Å) hydrogen bond in a centrosymmetric manner to form a tetramer, as highlighted in purple in Fig. 7b. With the engagement of HT, the tetramers are connected by $O_3\text{-H}\cdots O_2$ (d = 2.763 Å) and $N_2\text{-H}\cdots O_3$ (d = 2.882 Å) to form a serrated 2D layer parallel to the bOc

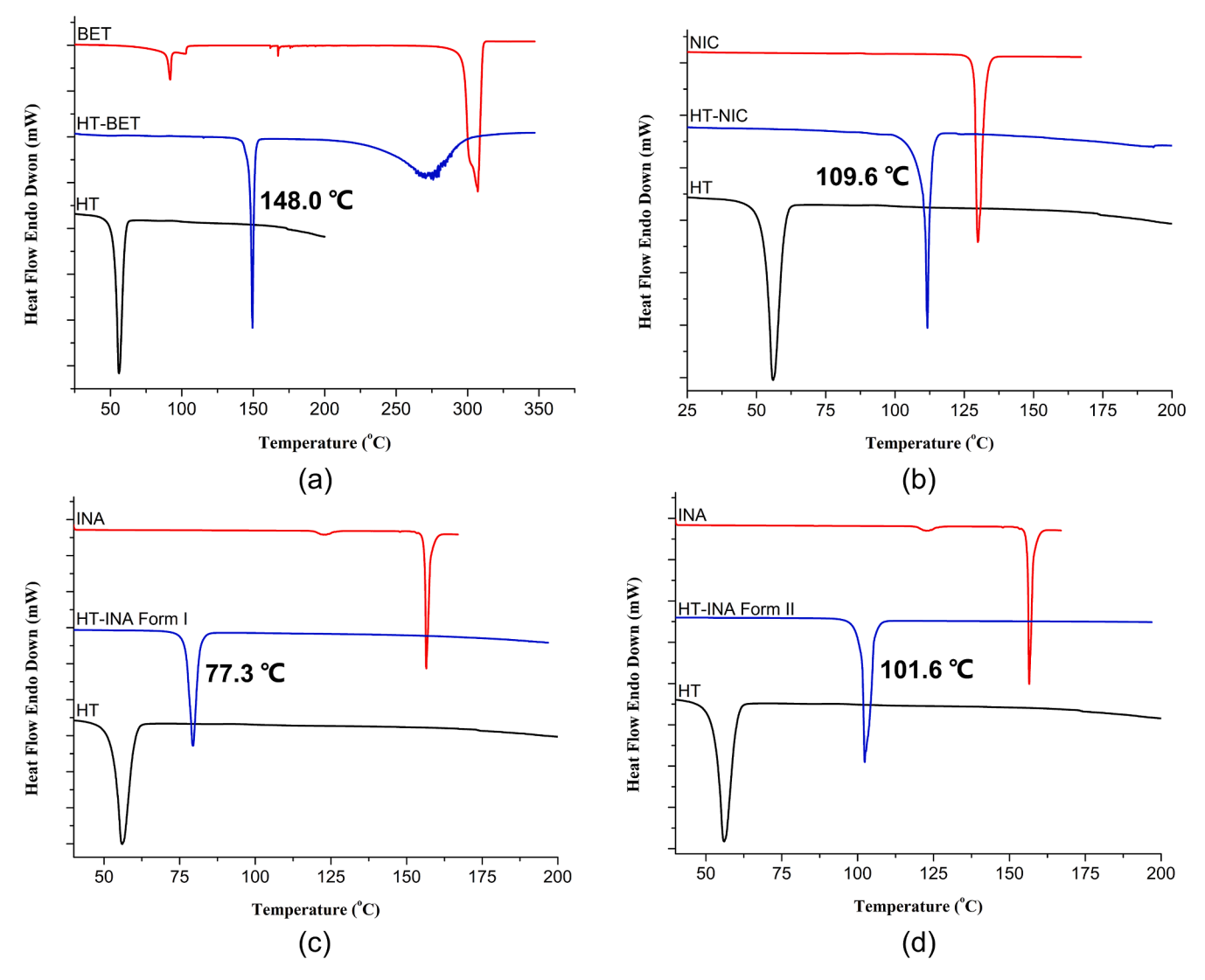


Fig. 8. DSC profiles of HT, HT cocrystals and the corresponding coformers: (a) HT-BET, (b) HT-NIC, (c) HT-INA Form I, and (d) HT-INA Form II. The onset temperature of HT cocrystals is labeled on each graph.

 Table 2

 Comparison between polymorphs of HT-INA cocrystal.

	Form I	Form II
Melting point (onset, °C)	77.3	101.6
Enthalpy of transition (J·g ⁻¹)	147.4	165.4
Calculated density (g·cm ⁻³)	1.333	1.393
Packing fraction (%)	68.4	71.5

plane. The 2D layers are further connected by O_3 -H··· O_2 (d = 2.763 Å) and N_2 -H··· O_3 (d = 2.882 Å) hydrogen bonds to form the spatial structure of HT-INA Form II (Fig. 7c).

3.3. Thermal analysis

The DSC curves and the onset melting temperature of HT cocrystals and corresponding coformers are presented in Fig. 8. The overlaid TGA and DSC curves of the cocrystals are shown in Fig. S3. All cocrystals are non-solvated since no weight loss steps appear before the melting events according to the TGA results. HT-BET, HT-NIC, HT-INA Form I, and HT-INA Form II show sharp melting peaks at onset temperature of 148.0 $^{\circ}\text{C}$, 109.6 $^{\circ}\text{C}$, 77.3 $^{\circ}\text{C}$, and 101.6 $^{\circ}\text{C}$, respectively, significantly higher than that of HT (53.2 $^{\circ}\text{C}$). As shown in Table 2, HT-INA Form II

exhibits higher onset temperature, melting enthalpy and packing

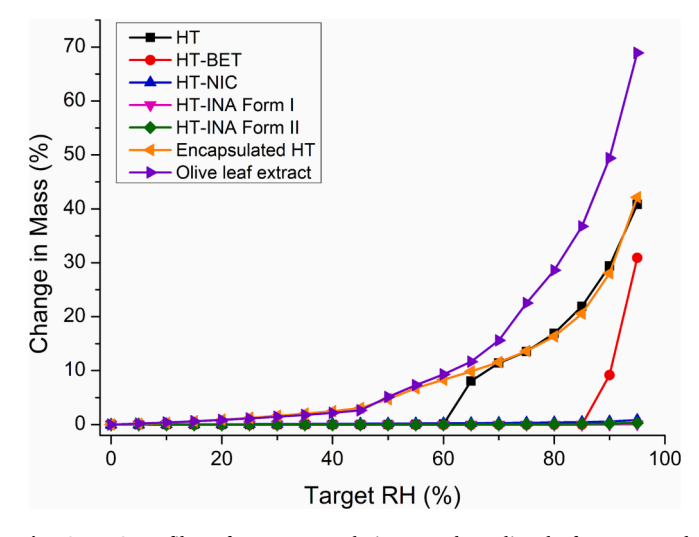


Fig. 9. DVS profiles of HT, encapsulation powder, olive leaf extract and HT cocrystals.

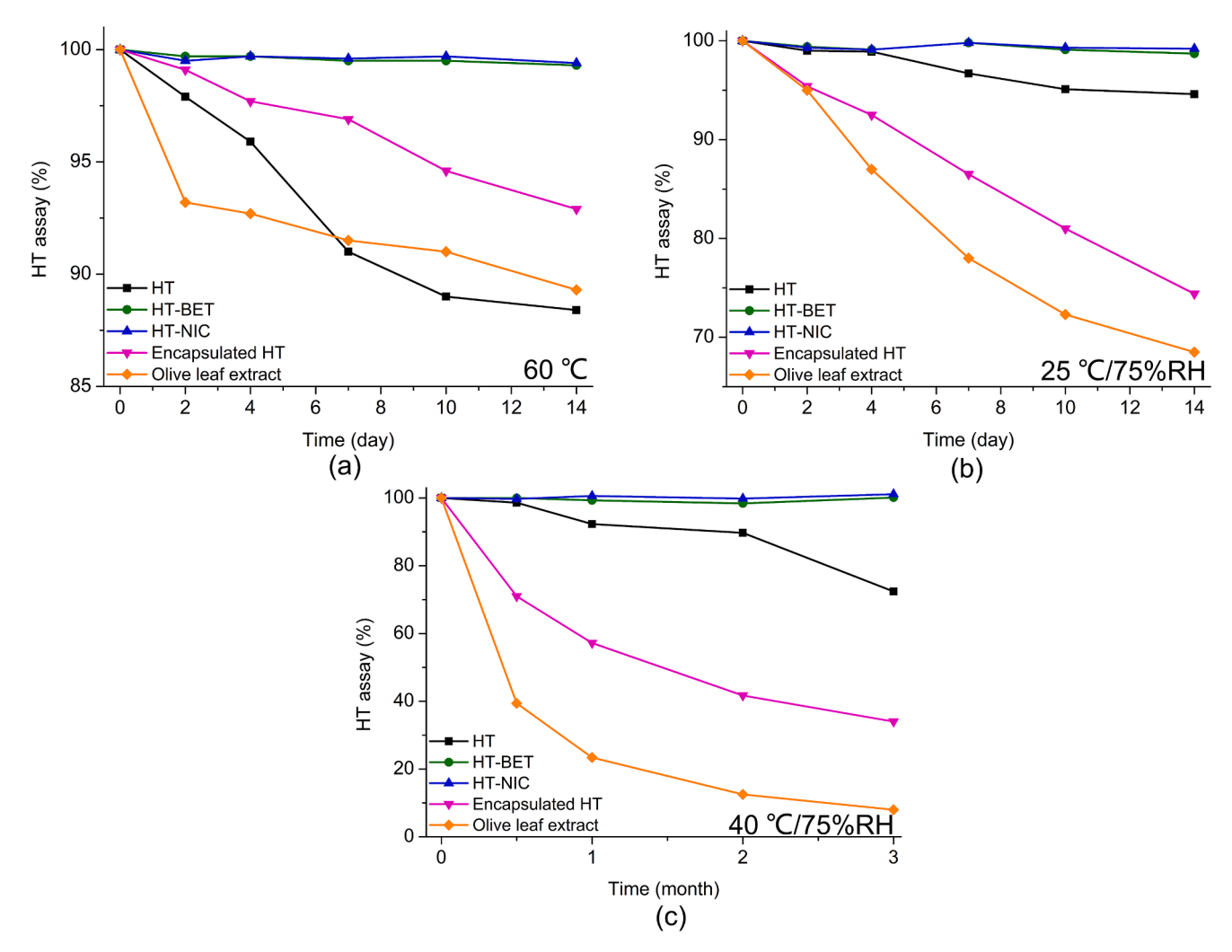


Fig. 10. Chemical stability of HT, HT cocrystals, encapsulated HT powder and olive leaf extract under (a) high temperature (60 °C), (b) high humidity (75%RH), and (c) accelerated conditions (40 °C/75%RH).

fraction than HT-INA Form I. They are monotropic related according to heat-of-fusion rule (Burger and Ramberger, 1979). Additionally, when equimolar of HT-INA Form I and HT-INA Form II was suspended in organic solvents such as ethyl acetate, methyl tert-butyl ether and methyl isobutyl ketone at room temperature for 24 h, the mixture was eventually converted to HT-INA Form II. This indicates that HT-INA Form II is thermodynamically favorable. It is noteworthy that the melting point difference is remarkable (more than 20 $^{\circ}$ C) between the two forms, which could indicate a high metastability for Form I.

3.4. Hygroscopicity

HT is very easy to absorb water and becomes oily liquid thereafter. Although it can be converted to flowable powder using encapsulation technique, the hygroscopicity is aggravated. The water sorption kinetics of HT, HT encapsulation powder, olive leaf extract rich in HT, and four HT cocrystals are monitored by DVS and the results are presented in Fig. 9. In the case of encapsulated HT and olive leaf extract, the water uptake increases continuously with relative humidity, reaching 2.5 % and 3.8 % at 40 % RH. At 80 % RH, water uptake even reaches 16.5 % and 28.6 % respectively. For pure HT, no significant weight gain is observed below 60 % RH (<0.1 %). However, the hygroscopicity increases dramatically when exposed to over 60 % RH. The water absorption of HT is as high as 16.9 % at 80 % RH, which is as high as HT encapsulation powder. In the case of HT-BET cocrystal, water uptake is

negligible in the range of 0–85 %, but significantly increase when relative humidity is above 85 %. Notably, cocrystals of HT-NIC, HT-INA Form I and HT-INA Form II are moisture resistant in the range of 0–95 % RH, with less than 1 % weight gain at 95 % RH. Therefore, cocrystallization is much more effective than encapsulation in reducing the hygroscopicity of HT.

3.5. Chemical stability

Hydroxytyrosol is extremely sensitive to oxidation, which is a big concern in its application in nutraceutical industry. Cocrystallization significantly increases its melting point and decreases its hygroscopicity, which underlies improved stability. Herein, the thermal (60 °C), humidity (75 %RH) and accelerated stability (40 °C/75 %RH) were investigated for pure HT, olive leaf extract, encapsulated HT powder, and two edible cocrystals HT-BET and HT-NIC. The assays of HT during stability tests are summarized in Table S1. In the context of high temperature (Fig. 10a), obvious degradation was observed in pure HT, olive leaf extract and encapsulated HT, and the assay of HT dropped to 88.4 %, 89.3 %, and 92.9 % respectively after 14 days. The stability under 75 % RH has great correlation with the extent of moisture uptake (Table S2). Olive leaf extract and encapsulated HT absorb water more than 17 % under 75 % RH. And the assay of HT is only 68.5 % and 74.4 % after 14 days. Pure HT was more resistant to high humidity and 94.6 % was left after 14 days. Notably, no obvious changes in HT content were observed in both conditions for the two cocrystals. Furthermore, accelerated stability was conducted for three months, which shows significant difference between these HT forms (Fig. 10c). After three months, while olive leaf extract and encapsulated HT decreased to only 8.0 % and 34.0 %, pure HT is still up to 72.4 % and the two edible cocrystals show the best stability without any degradation.

4. Conclusion

The present study attempts to improve the physicochemical properties of the powerful antioxidant HT by solid-state modification. HT is deliquescent and chemically unstable. We have successfully obtained four cocrystals of HT for the first time, namely HT-BET, HT-NIC, HT-INA Form I and HT-INA Form II. All cocrystals are solid with good flowability at room temperature, wherein the melting point of HT-NIC and HT-BET are 55.6 °C and 94.0 °C higher than pure HT, respectively. Pure HT absorbs water easily and immediately turns into a dark red liquid, and its encapsulated formulation cannot survive at high humidity. After cocrystallization, hygroscopicity is dramatically reduced. While olive leaf extract and encapsulated HT absorbs more than 10 % water under 75 % RH, the water uptake of cocrystals is negligible. Moreover, stability under high temperature and humidity was also significantly improved after cocrystallization. Under accelerated condition, the two cocrystals remain unchanged after three months, which can be attributed to their higher melting point and lower hygroscopicity. Therefore, HT-NIC and HT-BET cocrystals can be considered as best-in-class HT source to be applied in the nutraceutical industry, regarding with their superior stability.

CRediT authorship contribution statement

Bingqing Zhu: Conceptualization, Data curation, Formal analysis, Funding acquisition, Investigation, Methodology, Validation, Writing – review & editing. **Mengyuan Xia:** Conceptualization, Data curation, Methodology, Formal analysis, Investigation, Writing – original draft. **Zhenfeng Ding:** Investigation. **Xiaoyi Rong:** Investigation, Data curation. **Xuefeng Mei:** Supervision, Project administration, Resources.

Declaration of Competing Interest

The authors declare that they have no known competing financial interests or personal relationships that could have appeared to influence the work reported in this paper.

Data availability

No data was used for the research described in the article.

Acknowledgement

We thank the Shanghai Sailing Program (Grants 20YF1457400) for funding.

Appendix A. Supplementary data

Supplementary data to this article can be found online at https://doi.org/10.1016/j.ijpharm.2023.123470.

References

- Bofill, L., de Sande, D., Barbas, R., Prohens, R., 2021. A new and highly stable cocrystal of vitamin D3 for use in enhanced food supplements. Cryst. Growth Des. 21, 1418–1423.
- Burger, A., Ramberger, R., 1979. On the polymorphism of pharmaceuticals and other molecular crystals. II. Microchimica Acta 72, 273–316.
- Dias, J.L., Lanza, M.R., Ferreira, S.R.S., 2021. Cocrystallization: A tool to modulate physicochemical and biological properties of food-relevant polyphenols. Trends Food Sci. Technol. 110, 13–27.
- Galmes, S., Reynes, B., Palou, M., Palou-March, A., Palou, A., 2021. Absorption, distribution, metabolism, and excretion of the main olive tree phenols and polyphenols: A literature review. J. Agric. Food Chem. 69, 5281–5296.
- Gonzalez, E., Gomez-Caravaca, A.M., Gimenez, B., Cebrian, R., Maqueda, M., Martinez-Ferez, A., Segura-Carretero, A., Robert, P., 2019. Evolution of the phenolic compounds profile of olive leaf extract encapsulated by spray-drying during in vitro gastrointestinal digestion. Food Chem. 279, 40–48.
- Gullon, P., Gullon, B., Astray, G., Carpena, M., Fraga-Corral, M., Prieto, M.A., Simal-Gandara, J., 2020. Valorization of by-products from olive oil industry and added-value applications for innovative functional foods. Food Res. Int. 137, 109683.
- Loizzo, M.R., Lecce, G.D., Boselli, E., Menichini, F., Frega, N.G., 2011. Inhibitory activity of phenolic compounds from extra virgin olive oils on the enzymes involved in diabetes, obesity and hypertension. J. Food Biochem. 35, 381–399.
- Lopez de las Hazas, M.C., Pinol, C., Macia, A., Romero, M.-P., Pedret, A., Sola, R., Rubio, L., Motilva, M.-J., 2016. Differential absorption and metabolism of hydroxytyrosol and its precursors oleuropein and secoiridoids. J. Funct. Foods 22, 52–63
- Lopez de las Hazas, M.C., Godinho-Pereira, J., Macia, A., Almeida, A.F., Ventura, M.R., Motilva, M.J., Santos, C.N., 2018. Brain uptake of hydroxytyrosol and its main circulating metabolites: Protective potential in neuronal cells. J. Funct. Foods 46, 110–117.
- Mentella, M.C., Scaldaferri, F., Ricci, C., Gasbarrini, A., Miggiano, G.A.D., 2019. Cancer and mediterranean diet: A review. Nutrients 11.
- Monteiro, M., Silva, A.F.R., Resende, D., Braga, S.S., Coimbra, M.A., Silva, A.M.S., Cardoso, S.M., 2021. Strategies to broaden the applications of olive biophenols oleuropein and hydroxytyrosol in food products. Antioxidants (basel). 10.
- Rosato, V., Temple, N.J., La Vecchia, C., Castellan, G., Tavani, A., Guercio, V., 2019. Mediterranean diet and cardiovascular disease: a systematic review and metaanalysis of observational studies. Eur. J. Nutr. 58, 173–191.
- Wang, N., Xie, C., Lu, H., Guo, N., Lou, Y., Su, W., Hao, H., 2018. Cocrystal and its application in the field of active pharmaceutical ingredients and food ingredients. Curr. Pharm. Des. 24, 2339–2348.